Journal of Marine Science and Technology

Volume 16 | Issue 1 Article 5

DESIGN AND IMPLEMENTATION OF AN ALL-DIGITAL REAL-TIME UNDERWATER ACOUSTIC TRANSCEIVER USING DIGITAL SIGNAL PROCESSORS

Fu-Sheng Lu
Department of Computer and Communication Engineering, St. John's University, Taipei County, Taiwan, R.O.C., lufs@mail.sju.edu.tw

Ching-Hsiang Tseng
Department of Electrical Engineering, National Taiwan Ocean University, Keelung, Taiwan, R.O.C.

Bin-Chong Wu
Smart Phone R&D Division, Arima Communications Corp., Taiwan, R.O.C.

Recommended Citation

Lu, Fu-Sheng; Tseng, Ching-Hsiang; and Wu, Bin-Chong (2008) "DESIGN AND IMPLEMENTATION OF AN ALL-DIGITAL REAL-TIME UNDERWATER ACOUSTIC TRANSCEIVER USING DIGITAL SIGNAL PROCESSORS," *Journal of Marine Science and Technology*: Vol. 16: Iss. 1, Article 5.
DOI: 10.51400/2709-6998.1995
Available at: https://jmstt.ntou.edu.tw/journal/vol16/iss1/5

DESIGN AND IMPLEMENTATION OF AN ALL-DIGITAL REAL-TIME UNDERWATER ACOUSTIC TRANSCEIVER USING DIGITAL SIGNAL PROCESSORS

Fu-Sheng Lu*, Ching-Hsiang Tseng**, and Bin-Chong Wu***

Key words: underwater acoustic communication, direct-sequence spread spectrum, delay-locked loop, synchronization, decision-feedback equalizer, digital signal processor.

ABSTRACT

In this paper, an all-digital transceiver for real-time underwater acoustic (UWA) communications is developed using digital signal processors (DSPs). The design of the transceiver is based on the direct-sequence spread-spectrum (DS/SS) modulation scheme, in which the timing synchronization is efficiently achieved by employing a sliding correlator and a modified noncoherent delay-locked loop for code acquisition and tracking, respectively. In addition, an equal-gain combiner (EGC) and an adaptive decision-feedback equalizer (DFE) are included in the receiver to enhance its interference rejection capability under multipath fading environments. Several real-time UWA transmission tests are conducted in an experimental water tank to evaluate the performance of the transceiver. The test data include plain text and simple image files. The test result shows that reliable real-time UWA communications can be accomplished by the proposed transceiver.

I. INTRODUCTION

The UWA communication channel is generally considered as an unfavorable and difficult environment for data transmission. Its multipath fading and Doppler spreading effects make the building of a reliable UWA communication system a challenging task. Most commercially available UWA communication systems developed so far use noncoherent modulation schemes like the frequency shift keying (FSK) for simplicity. However, as the hardware technology progresses, the focus of the UWA communication research has been shifted toward more complicated coherent modulation schemes such as phase shift keying (PSK) and quadrature amplitude modulation (QAM) [6, 13]. Furthermore, the design of UWA transceivers has been revolutionized over the past few years due to the tremendous advances in DSP technology [2, 7, 18, 22]. The digital VLSI offers communication engineers a platform to realize algorithms that were frequently inconceivable in the analog domain. Specifically, Choi *et al.* [1, 2] presented a design of phase-coherent all-digital UWA transceiver whose frame synchronization method requires neither a phase-locked loop (PLL) nor a delay-locked loop (DLL), and the operation of the transceiver relies largely on the adaptive equalizer and the Viterbi decoding algorithm. Trubuil *et al.* [18] developed a real-time high data rate UWA communication link, where a self-optimized configuration multiple input decision feedback equalizer (SOC-MI-DFE) was proposed and implemented on a TMS320 C6201 DSP module. These all-digital implementations require the sampling of the received signal to be synchronized to the incoming symbols. Interpolation methods for achieving such synchronization have also been proposed by several researchers [9, 21].

Recently, the SS technique was found to be more suitable for UWA communications in the sense that it can achieve reliable transmission by suppressing detrimental effects like jamming, interference from other users, and multipath propagation. In addition, the SS method can also provide multiple access capability in systems shared by many users. This will serve as a basis for future undersea networks [3, 20]. There are various designs for SS-based UWA communication systems that can be found in the literature [3, 8, 12, 14, 15, 19, 20]. These designs, however, require receivers with sophisticated signal processing algorithms, which in turn demand high-end (and hence high cost) DSPs. This makes them less favorable in situations where lowering the implementation cost is of great concern.

In this paper, a simple design with computationally efficient algorithms is proposed to implement an all-digital transceiver for DS/SS-based UWA communication systems. In this design, the spreading code acquisition is achieved by employing a sliding correlator to process the received signal. By locating the peaks of the correlator filter output signal, the spreading code timing can be coarsely estimated. The coarsely synchronized signal is further processed by a modified noncoherent DLL for

Paper submitted 11/06/06; accepted 02/26/07. Author for correspondence: Fu-Sheng Lu (e-mail: lufs@mail.sju.edu.tw).

** Department of Computer and Communication Engineering, St. John's University, Taipei County, Taiwan, R.O.C.*

*** Department of Electrical Engineering, National Taiwan Ocean University, Keelung, Taiwan, R.O.C.*

**** Smart Phone R&D Division, Arima Communications Corp., Taiwan, R.O.C.*

code tracking to attain the fine-tuned synchronization. To combat the multipath fading effects of the UWA communication channel, we adopt the diversity and the equalization techniques. An equal-gain combination diversity scheme [4, 11] and a decision-directed DFE (DD-DFE) are incorporated in the receiver. The transmitter and the receiver are implemented on two separate TMS320 C6711 DSP starter kit (DSK) modules. The goodness of the designed transceiver is tested on an acrylic water tank mimicking an actual UWA channel. Note that the glassy walls of the water tank suggest that the experimental channel is highly reverberant and suffers from severe interference. Nevertheless, the designed transceiver is able to accomplish reliable transmission of data in real time.

II. THE TRANSCEIVER STRUCTURE

1. Transmitter

The bit stream to be transmitted is organized in frames as shown in Fig. 1. The preamble and the end code indicate the start and the end of a message frame, respectively. They are used by the receiver for the frame synchronization. The training sequence is used by the adaptive equalizer in the receiver for optimizing the equalizer coefficients. The information-bearing data follow the training sequence. The gap between the preamble and the training sequence is for ensuring the completion of the frame synchronization in the receiver before the reception of the training sequence.

The block diagram of the transmitter is illustrated in Fig. 2. The channel encoder employs the BCH code. The multiplexer adds the preamble, the training sequence, and the end code to the information bearing data to form a bit stream with the frame format shown in Fig. 1. The DS/SS modulator performs the QPSK modulation on the incoming bit stream and then multiplies the modulated signal with the spreading signal generated by a pseudo-random noise (PN) code generator. The digital-to-analog converter (DAC) converts the digital DS/SS signal to an analog signal. This signal, after being boosted by the power amplifier, is then passed to the UWA channel through the hydrophone.

2. Receiver

The block diagram of the receiver is illustrated in Fig. 3, where a hydrophone array with M sensors is shown. The M sets of data collected by the M sensors provide diversity to following stages of the receiver. After being boosted by the pre-amplifier, the received signals from the M sensors are over sampled by the analog-to-digital converter (ADC) and then passed to the EGC. The EGC increases the signal-to-noise power ratio and simplifies the computation in succeeding stages by combining the M received signals into one using the equal gain combining diversity technique [4, 11]. Following the EGC is the frame synchronization which is attained by correlation filtering. The timing synchronization block performs the spreading code acquisition and tracking. The code acquisition is conducted by convolving the received signal with a correlation filter. By locating the peaks of the filter output, one can roughly

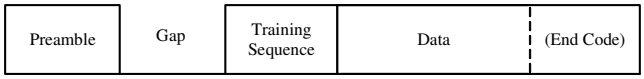

Fig. 1. The frame structure of the transmitted bit stream.

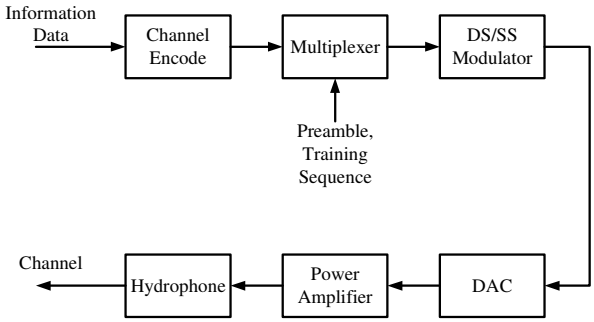

Fig. 2. Block diagram of the transmitter.

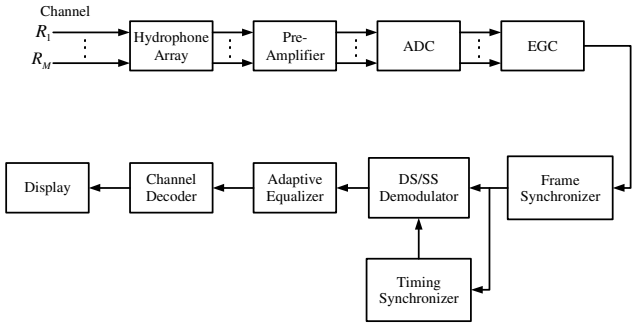

Fig. 3. Block diagram of the receiver.

synchronize the received signal with the locally generated spreading signal. The code tracking is performed by using a modified noncoherent DLL, which fine-tunes the alignment between the received signal and the locally generated spreading signal. The operation of the modified noncoherent DLL will be explained later. With the aid of the synchronized timing, the DS/SS signal can be despreaded and demodulated properly. The adaptive DD-DFE following the DS/SS demodulator is used to cancel the residual intersymbol interference (ISI) in the demodulated signal. The channel decoder performs the BCH decoding to correct potential data errors caused by the channel impairments.

III. PROCESSING TECHNIQUES

1. Synchronization Schemes

The purpose of timing synchronization is to allow the locally generated spreading signal to synchronize with the one embedded in the received signal. The timing synchronization is usually achieved in two stages: code acquisition and code tracking. The code acquisition is used to bring the timing offset between the received signal and the locally generated spreading signal to within the pull-in range of the code tracking loop, and

then the code tracking can be initiated to correct the timing offset.

The block diagram of the code acquisition process is depicted in Fig. 4, where a sliding correlator is used as a matched filter [10]. The control circuit adjusts the timing alignment between the locally generated spreading signal and the received signal. When the timing alignment is correct, the correlator output will reach its maximal value. Therefore, the code acquisition can be attained by examining the peak locations of the correlator output signal.

The code tracking process can be accomplished by using a noncoherent DLL [10]. In this paper, we introduce a modified noncoherent DLL which is slightly different from the conventional one. The block diagram of the proposed modified noncoherent DLL is given in Fig. 5. In the modified version, the local spreading signal generator provides only one specific signal $p(t)$, and the received signal is shifted to yield the early and the late signals. The displacements of the shifting are controlled by the voltage-controlled oscillator (VCO). This process can be conducted by using the intrinsic registers of the DSP module and therefore can be easily implemented.

The operation of the modified noncoherent DLL is explained as follows. Suppose that the baseband signal at the transmitting end is denoted by $b(t)$, then $b(t)$ can be expressed as

$$b(t) = \sum_{k=-\infty}^{\infty} b_k P_b(t - kT_b) \tag{1}$$

where $b_k = \pm 1$ is the kth data bit, $P_b(t)$ is the impulse response of the pulse shaping filter at the transmitter, and T_b is the bit duration. In this case, the DS/SS signal appears at the receiving end can be written as

$$S_r(t) = b(t-\tau)c(t-\tau)\cos(2\pi f_c t + \varphi(t)) \tag{2}$$

where $c(t)$ is the spreading code signal, f_c is the carrier frequency, τ is the propagation delay time, and $\varphi(t)$ is the random phase.

The signal $p(t)$ generated by the local spreading signal generator can be written as follows:

$$p(t) = 2c(t)\cos(2\pi f_c t) \tag{3}$$

Let $\delta^- = \hat{\tau} - \frac{\Delta}{2}T_c$ and $\delta^+ = \hat{\tau} + \frac{\Delta}{2}T_c$, where $\hat{\tau}$ is the estimated value of the propagation delay time, Δ is the designated separation time between the early and the late signals, and T_c is the chip duration. In this case, the signals $x_1(t)$ and $x_2(t)$ in Fig. 5 can be expressed as

$$\begin{aligned} x_1(t) &= S_r(t+\delta^-)p(t) \\ &= b(t-\tau+\delta^-)c(t)c(t-\tau+\delta^-) \\ &\times[\cos(2\pi f_c(\delta^-) + \varphi(t+\delta^-)) \\ &+ \cos(4\pi f_c t + 2\pi f_c(\delta^-)) + \varphi(t+\delta^-))] \end{aligned}$$

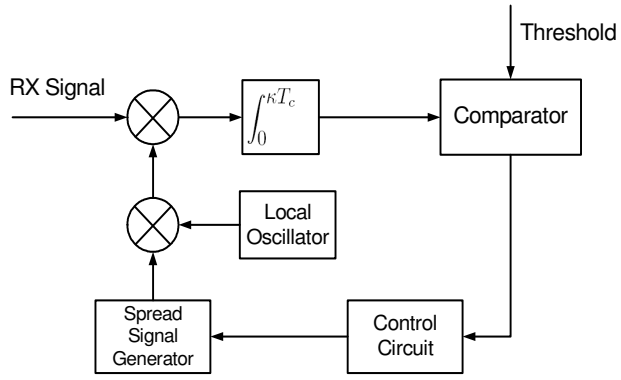

Fig. 4. The block diagram of the code acquisition process.

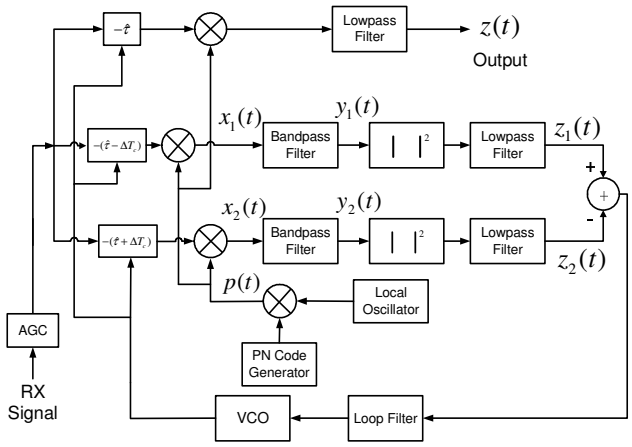

Fig. 5. The block diagram of the modified noncoherent DLL.

$$\begin{aligned} x_2(t) &= S_r(t+\delta^+)p(t) \\ &= b(t-\tau+\delta^+)c(t)c(t-\tau+\delta^+) \\ &\times[\cos(2\pi f_c(\delta^+) + \varphi(t+\delta^+)) \\ &+ \cos(4\pi f_c t + 2\pi f_c(\delta^+)) + \varphi(t+\delta^+))]. \end{aligned} \tag{4}$$

Note that the center frequency of the bandpass filters in Fig. 5 is $2f_c$. If the bandwidth of the bandpass filters is narrow enough, only the DC component of the spreading waveform product $c(t)c(t-\tau+\delta^-)$ (or $c(t)c(t-\tau+\delta^+)$) in $x_1(t)$ (or $x_2(t)$) can survive the bandpass filtering process [10]. Note that the DC component of the spreading waveform product is the autocorrelation function of the spreading waveform. Consequently, the signals $y_1(t)$ and $y_2(t)$ in Fig. 5 are

$$y_1(t) = b(t-\tau+\delta^-)R_c(\tau-\delta^-)\cos(4\pi f_c t + \varphi_1(t)) \tag{5}$$

$$y_2(t) = b(t-\tau+\delta^+)R_c(\tau-\delta^+)\cos(4\pi f_c t + \varphi_2(t)) \tag{6}$$

where $R_c(t)$ is the autocorrelation of the spreading waveform $c(t)$, $\varphi_1(t) = 2\pi f_c(\delta^-) + \varphi(t+\delta^-)$, and $\varphi_2(t) = 2\pi f_c(\delta^+)$

$+\varphi(t+\delta^+)$.

Furthermore, notice that

$$y_1^2(t) = R_c^2(\tau-\delta^-)\left[\frac{1+\cos(8\pi f_c t+2\varphi_1(t))}{2}\right] \tag{7}$$

$$y_2^2(t) = R_c^2(\tau-\delta^+)\left[\frac{1+\cos(8\pi f_c t+2\varphi_2(t))}{2}\right] \tag{8}$$

The signals $z_1(t)$ and $z_2(t)$ in Fig. 5 are obtained by lowpass filtering the signals $y_1^2(t)$ and $y_2^2(t)$, respectively. Therefore, one can easily see from (7) and (8) that

$$z_1(t) = R_c^2(\tau-\hat{\tau}+\frac{\Delta}{2}T_c) \tag{9}$$

$$z_2(t) = R_c^2(\tau-\hat{\tau}-\frac{\Delta}{2}T_c) \tag{10}$$

The result matches exactly with that obtained by the conventional noncoherent DLL [10]. This shows that the modified noncoherent DLL is equivalent to the conventional noncoherent DLL in terms of the functionality. However, we found that the modified noncoherent DLL is a bit simpler to implement on the DSK module. Therefore, we adopt the modified noncoherent DLL in our design. Note that the difference between the two signals $z_1(t)$ and $z_2(t)$ is an indication of the goodness of the propagation delay time estimate $\hat{\tau}$. This difference signal, after being smoothed by the loop filter, is used by the VCO to adjust the time delay $\hat{\tau}$.

Note that, to increase the stability of the DLL operation, an automatic gain control (AGC) mechanism is used to control the dynamic range of the input signal to the DLL (see Fig. 5) [16].

The frame synchronization can also be achieved by correlating the spreading code signal with the received signal. Recall that a preamble is added to the beginning of a frame. The frame synchronizer first uses the same code acquisition process as that shown in Fig. 4 to align the timing between the locally generated spreading signal and the received preamble signal. Once proper alignment is achieved, a peak will appear in the correlation filter output signal. If the preamble is 2-bit long, then two prominent peaks will appear at the output of the correlation filter every time the spreading signal is properly aligned with a preamble. As an example, the preamble waveform of a BPSK modulated DS/SS signal with a bit rate of 302 bits/sec and a sampling rate of 150k Hz is shown at the top of Fig. 6, while its corresponding correlation filter output is shown at the bottom of Fig. 6. The frame synchronization can be obtained by recognizing these peaks.

2. Adaptive Equalization

Equalization can compensate for the ISI resulting from the multipath fading effects of UWA channels. Several researchers have proposed various adaptive equalizers in their developments of underwater communication systems [2, 9, 14, 18, 23]. In this paper, we employ a simple DD-DFE for its effectiveness in diminishing the ISI caused by multipath fading effects of UWA channels [23]. The block diagram of the DD-DFE is shown in Fig. 7.

The DFE output $y(n)$ can be expressed as

$$\begin{aligned} y(n) &= \sum_{k=0}^{M-1} c_k(n)u(n-k) + \sum_{i=1}^{N} b_i(n)d(n-i) \\ &= \mathbf{c}^T(n)\mathbf{u}(n) + \mathbf{b}^T(n)\mathbf{d}(n-1) \end{aligned} \tag{11}$$

where $c_k(n)$ and $u(n-k)$, $k = 0,1, ..., M-1$, are the tap weights and the tap inputs of the feed-forward filter, respectively. The column vectors $\mathbf{c}(n)$ and $\mathbf{u}(n)$ include all the tap weights and the tap inputs of the feed-forward filter, respectively. In addition, $b_i(n)$ and $d(n-i)$, $i = 1, 2, ..., N$, are the tap weights and the tap decisions of the feedback filter, respectively. The column vectors $\mathbf{b}(n)$ and $\mathbf{d}(n-1)$ include all the tap weights and the tap inputs of the feedback filter, respectively. Define the composed tap weight vector $\mathbf{w}(n)$ as

$$\mathbf{w}(n) = [\mathbf{c}^T(n) \quad \mathbf{b}^T(n)]^T \tag{12}$$

and the composed input vector $\mathbf{x}(n)$ as

$$\mathbf{x}(n) = [\mathbf{u}^T(n) \quad \mathbf{d}^T(n-1)]^T \tag{13}$$

Using (12) and (13), one can rewrite (11) as $y(n) = \mathbf{w}^T(n)\mathbf{x}(n)$. The error signal of the DFE is given by

$$e(n) = d(n) - y(n) \tag{14}$$

The optimum filter coefficients can be estimated by minimizing the sum of weighted error squares

$$J(n) = \sum_{k=1}^{n} \lambda^{n-k} \left| d(k) - \mathbf{w}^T(n)\mathbf{x}(k) \right|^2 \tag{15}$$

where λ is the forgetting factor. The recursive least-squares (RLS) algorithm [5, 23] can be applied to adaptively minimizing (15).

3. Diversity

Diversity techniques, which are widely used for combating multipath fading effects, can be implemented in many ways. In this paper, we adopt a relatively simple yet effective spatial diversity technique called equal gain combining (EGC). The EGC combines the received signals from multiple hydrophones at different spatial locations to form a signal with a higher signal-to-noise ratio (SNR). Suppose that M receiving hydrophones are available. Let the received signal from the i-th hydrophone be denoted by $r_i(t)$, we have

$$r_i(t) = A_i e^{j\theta_i} s(t) + n_i(t), \quad i = 1, 2, ..., M \tag{16}$$

where $s(t)$ is the transmitted signal, $A_i e^{j\theta_i}$ is the fading factor for the receiving path of the i-th hydrophone, and $n_i(t)$ is the noise received by the i-th hydrophone. The output of the EGC can be written as follows:

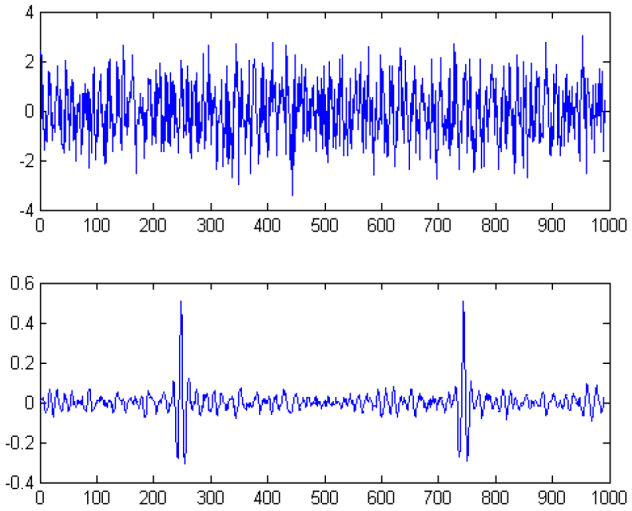

Fig. 6. The DS/SS preamble signal (top) and its corresponding correlation filter output (bottom). The abscissa is time in samples.

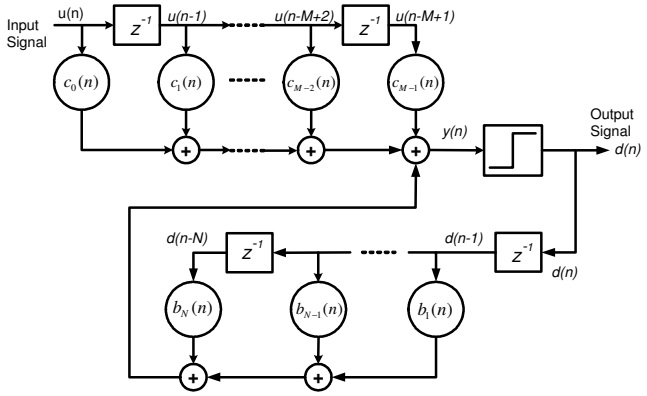

Fig. 7. The block diagram of the DD-DFE.

$$y(t) = \sum_{i=1}^{M} w_i r_i(t) \tag{17}$$

where $w_i = e^{-j\hat{\theta}_i}$ is the weight parameter for the i-th hydrophone. The EGC manages to co-phase the signals from the M hydrophones and then sums them up in a constructive way. When the M received signals are properly co-phased (i.e., $\hat{\theta}_i = \theta_i$ for $i = 1, 2, ..., M$), the SNR of the resulting EGC output signal is higher than those of the individual received signals.

IV. SIMULATION

To test the effectiveness of the proposed transceiver under fading environments, we conducted a simulation using a five-ray Rayleigh fading channel model [11]. The channel model is shown in Fig. 8, where $\alpha_i e^{j\phi_i}$ denotes the Rayleigh fading factor for the i-th ray, and τ_i denotes the time delay for

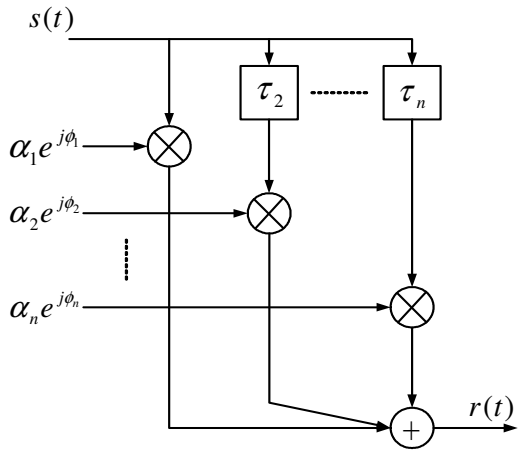

Fig. 8. The multi-ray Rayleigh fading channel model.

Table 1. Comparison of bit error rates for the simulation.

Number of receivers	without equalization	with equalization	with BCH code
1	1.3×10^{-1}	8.8×10^{-3}	3.5×10^{-3}
2	1.2×10^{-1}	3.1×10^{-4}	1.1×10^{-4}

the i-th ray. The time delays were chosen to be on the order of several symbol durations so the resulting channel could be characterized a frequency selective fading channel.

In this simulation, we utilized a DS/SS QPSK modulation with a 7-bit PN code. A (15, 11) BCH error correction code was employed. The carrier frequency was 24 kHz, the sampling rate was 384 kHz, the symbol rate was 1985 symbols/sec, and the SNR was set to 9 dB. The simulation result is shown in Table 1. We see that, for the one receiver case, the bit error rate (BER) without using the equalizer is 0.13. With the aid of the equalizer, the BER is lowered by two orders of magnitude to 8.8×10^{-3}. Adding the BCH code further lowers the BER. The result for using two receivers with the EGC technique is also shown in Table 1. We see the EGC technique does improve the BER performance.

V. IMPLEMENTATION

Two Texas Instruments TMS320 C6711 DSK modules [17], together with an ADC and a DAC, are used to build up the proposed all-digital transceiver. The integrated circuit chips AD7891-1 and DAC8462 of Analog Devices are used as the ADC and the DAC, respectively, in the transceiver. The flowcharts for the transmitter and the receiver programs are shown in Figs. 9 and 10, respectively.

In the transmitter program, either a plain text file or a simple image file is read and then converted to binary to form a bit stream. This bit stream, after being encoded with a (7,4) BCH

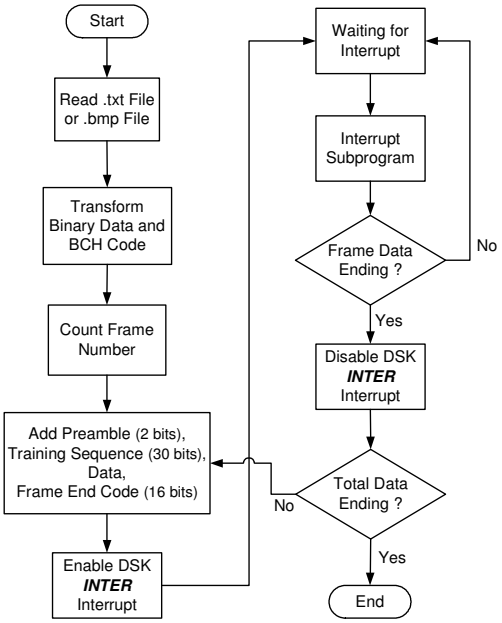

Fig. 9. Flowchart for the transmitter program.

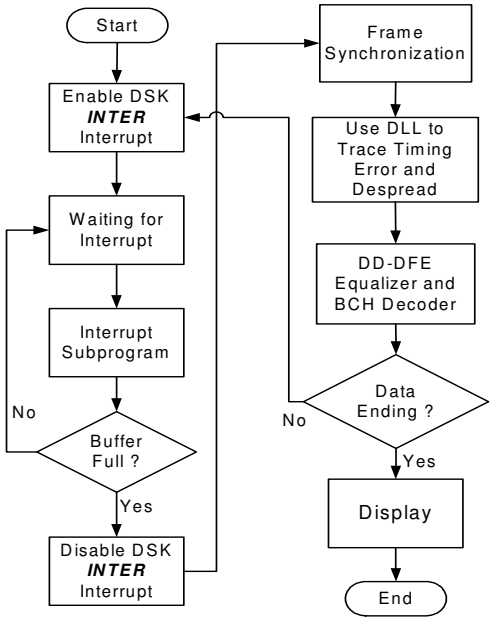

Fig. 10. Flowchart for the receiver program.

code, is further divided into frames. The preamble, the training sequence, and the end code are added to each frame according to Fig. 1. Once a frame is ready, the transmitter program enables the internal interrupt function of the transmitter DSK module and then waits for the interrupt. An interrupt will start the transmitter interrupt subprogram, whose flowchart is shown in Fig. 11(a). In the transmitter interrupt subprogram, first the DAC is enabled, and then the waveform corresponding to the current symbol is determined. To improve the computational efficiency of the subprogram, the sample values of the QPSK waveforms are pre-calculated and stored as a table in the transmitter DSK module for fast accessing. The current sample value of the selected waveform is sent to the DAC for generating the corresponding analog waveform before the transmitter subprogram ends. The rate of the interrupt (i.e., the sampling rate) can be controlled by setting the value of the timer period register. Note that the carrier frequency and the clock source frequency are related as follows:

$$f_c = (\frac{f_{cs}}{k}) \times \frac{1}{N} \ (Hz) \tag{18}$$

where f_c is the carrier frequency of the QPSK, N is the desired number of samples in one cycle, f_{cs} is the clock source frequency, and k is the value of the timer period register. The clock source frequency is one quarter of the CPU frequency. The CPU frequency for the TMS320 C6711 DSK is 150 MHz, which means $f_{cs} = f_{\text{CPU}} / 4 = 37.5 \times 10^6$ Hz. Given f_c, N, and f_{cs}, the value k of the timer period register can be calculated using (18).

After the transmitter interrupt subprogram is done with transmitting a sample, the transmitter main program checks whether the end of a frame is reached. If not, the main program will proceed to process the next sample by going back to wait for the interrupt, otherwise the main program will disable the DSK internal interrupt and start processing the next frame. The main program will end when all of the data frames are processed.

The receiver program (see Fig. 10) first enables the internal interrupt of the receiver DSK module and then waits for the interrupt. An interrupt will start the receiver interrupt subprogram, whose flowchart is shown in Fig. 11(b). The receiver interrupt subprogram enables the ADC and lets the ADC sample the received signal. The sampling rate of the ADC is also controlled by setting the timer period register value k in the receiver DSK module via (18). The receiver subprogram will check the validity of the sampled data to decide whether to save them in the data buffer or not. After the receiver subprogram ends, the receiver main program will check to see if the data buffer is full. If not, the receiver main program will go back to wait for the next interrupt, otherwise it will disable the internal interrupt of the receiver DSK module. A frame of data is resolved from the data buffer via the succeeding frame synchronization, code synchronization, de-spreading, equalizing, and BCH decoding processes. For enhancing the computational efficiency of the program, the sample values of the spreading signal required by the receiver are stored in the register for fast accessing. After the frame of data is retrieved, the main program is ready for processing the next frame of data and will go back to enable the internal interrupt unless the end of data is reached. Once the end of data is reached, the receiver main program will display the received data on the computer screen.

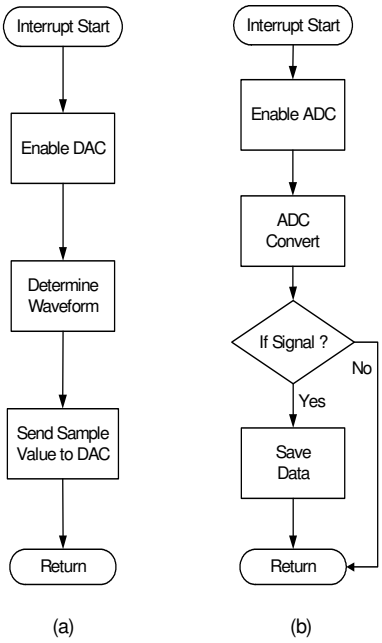

Fig. 11. (a) The transmitter and (b) the receiver interrupt subprograms.

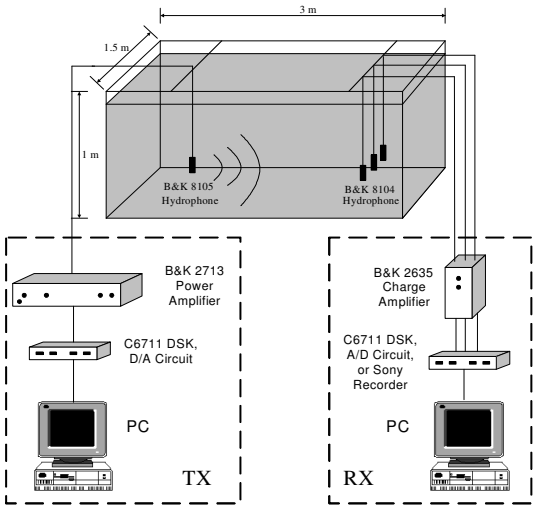

Fig. 12. The setup of the experimental equipments.

VI. EXPERIMENTS

To evaluate the goodness of the designed transceiver, transmitting and receiving experiments were conducted in the Underwater Communications Laboratory at National Taiwan Ocean University (NTOU). The setup of the experimental equipments is shown in Fig. 12. At the transmitter end, a B&K 2713 power amplifier was used to magnify the transmitted signal waveform, and a B&K 8103 hydrophone was used as a sound transmitter (projector). At the receiving end, three B&K 8104 hydrophones were employed as a wide-range measuring transducer, and the signals received by the hydrophones were

Fig. 13. The water tank used in the experiments.

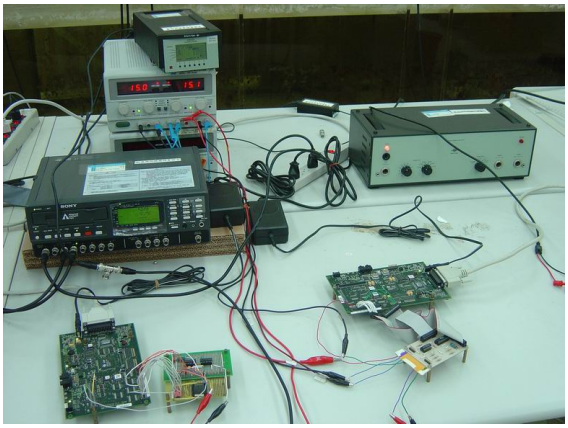

Fig. 14. The instruments used in the experiments.

filtered and boosted by a B&K 2635 charge amplifier. A cuboid-shaped acrylic water tank of size 3m(L) × 1.5m(W) × 1m(H) was used to mimic the actual UWA communication channel. Note that the water tank is not an anechoic tank. Its glassy surfaces yield strong reverberations which cause severe multipath fading effects. A picture of the water tank is shown in Fig. 13. A picture of the instruments used in the experiments is shown in Fig. 14, where two TMS320 C6711 DSK modules, one as the transmitter and the other as the receiver, are employed.

Due to the strong reverberations of the water tank, the intersymbol interference is in fact the dominating impairment of water tank channel. We found that increasing the power level of the transmitted signal could not significantly improve the system performance. Therefore, the power and noise levels are not specified in our experiments.

In all of the experiments, the carrier frequency is 18.750 kHz, the sampling rate is 150 kHz, the frame length is 224 bits/frame, and the data rate is 1,210 bits/sec. Since the QPSK modulation is adopted, the symbol rate is 605 symbols/sec. We used different PN codes for the preamble and the data. The spreading code for the preamble is a 32-bit PN sequence, while the one for the data is a 31-bit PN sequence.

National Taiwan Ocean University was originally established
in 1953 as a junior college for the study of maritime science
and technology. After eleven years, in 1964, we became a
maritime college which offered bachelor's and master's degrees
in various fields of maritime studies. During this period,
funds for running the college came from the Taiwan Provincial
Government of the Republic of China. In 1979 the national
government took over the funding and we became the National
Maritime College. After another decade, in1989, the college
grew into a full-fledged university,
National Taiwan Ocean University (NTOU).$

Fig. 15. The transmitted English text in the first experiment.

海大校訓:

誠：眞誠，實事求是，心存眞誠的態度。

樸：樸實，純樸耐勞，養成完整的人格。

博：博大，胸懷博大，培養寬宏的氣度。

毅：毅勇，堅毅茁壯，具備無畏的精神。

NTOU EE NDSP Lab

Fig. 16. The transmitted Chinese text in the first experiment.

Table 2. Comparison of bit error rates for the English text.

without equalization	with equalization	with BCH code
8.0×10^{-2}	2.2×10^{-3}	5.0×10^{-4}

In the first experiment, an English text file and a Chinese text file whose contents are shown in Figs. 15 and 16 were transmitted using the implemented TMS320 C6711 DSK transmitter. The three sets of signals collected by the three hydrophones were recorded using a SONY SIR-1000W data recorder. The three sets of data were combined into one by using the EGC diversity technique. The resulting signal was then demodulated, equalized, and decoded using the proposed techniques. The constellation of the received symbols before equalization is shown in Fig. 17(a), where the signal points are scattered and the separations of different signal states are obscure. Fig. 18 shows the detected English text without using equalization, and Fig. 19 shows the detected Chinese text without using equalization. We see that there are so many errors in the texts that the contents are incomprehensible. In contrast, Fig. 17(b) shows the signal constellation of the received symbols after equalization, where the signal points clearly congregate to form 4 groups centering near the designed 4 signal points of the QPSK. This makes the detected English text with equalization more legible, as shown in Fig. 20. The detected Chinese text with equalization is exactly the same as that shown in Fig. 16 (i.e., no error). Hence, it is not shown in a separate figure. The BERs for this experiment are compared in Table 2, where we see that the BER with equalization is an order of magnitude lower than that without equalization. Note that the above results were obtained

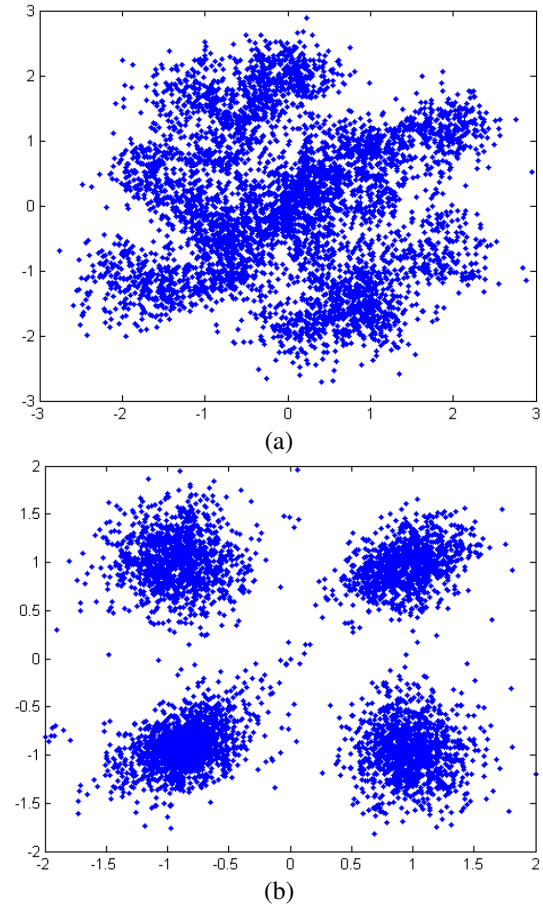

Fig. 17. Signal constellations for the received symbols (a) before and (b) after equalization.

麥tix~a|)Taiwa~)gcean)Univer■ity.was+origi~al|y)d■tabli■hed)
i~)1953-as(a)juniyr(callegi)fqr+the 蝶study(of)maritime)science)
and)technqligy.,After+eleven)years,$in)1964,'we)became)a
)maritime蝶ca|lege)which%offered)bachelir's(and)master's(degrees
in%variius(fields(of%maritime)studies. 蝶During+this |eriod,,
funds(far+running)the)ch1|ege)ca}e)f■j})the)Taiwa~)Orjvi~cial)
Gzve■n}e~t" af蝶the&Reyublic)tf)Chi~a.,in)1979.the!natiinal)
gyvernment tjak%over the)funding)and)we)became) theNatiinal)
Maritime)Cdllege.,After(anvther decade,.in1989,"the)cqllege)
grew+inth)afull-fledged 蝶university,,
natiinal)Taiwan)ocean)University((nT孢).$

Fig. 18. The detected English text without using equalization.

海大校訓:

誠咒眞誠呸實事求是，心存眞誠的態度咀

樸…樸實，純樸耐勞呸養成旦整的人格。

博呱博大，胸懷博大，培養寬宏j漁蠔蛎C

毅：毅勇，堅毅茁妨胞具備無畏的精神耶

NTOU EE FDSP Jab

Fig. 19. The detected Chinese text without using equalization.

```
▮ational Taiwan Ocean University was originally established
in 1953 as a junior college for the study of maritime science
and technology. After eleven years, in 1964, we became a
maritime college which offered bachelor's and master's degrees
in various fields of maritime studies. During this period,
funds for running the college came from the Taiwan Provincial
Government of the Republic of China. In 1979 the national
government took over the funding and we became the Nationa|
Maritime College. After andther decade, in1989, the college
grew into a full-fledgeduniversity,
National Taiwan Ocean University (NTOU).$
```

Fig. 20. The detected English text with equalization.

(a) (b)

Fig. 21. (a) The test image used in the second experiment and (b) the resolved image by the receiver.

without using the BCH encoding. When the BCH encoding was used in addition to the equalizer, the BER was lowered further by an order of magnitude. This result is also shown in Table 2. Based on this result, we included the equalizer and the BCH decoder in the receiver in the following experiments.

In the second experiment, the logo of NTOU shown in Fig. 21(a) was used as the test image. The transmitter and the receiver were exactly the same as those used in the first experiment. In Fig. 22, a segment of the transmitted signal waveform is shown at the top, while the corresponding received waveform is shown at the bottom. As expected, due to the severe mutipath effects and the noise, the received waveform looks quite different from the transmitted waveform. However, as shown in Fig. 21(b), the receiver was able to resolve the image properly. The achieved BER is 9.28×10^{-4}.

In the third experiment, the same NTOU logo image used in the second experiment was used as the test data. However, instead of using the SONY SIR-1000W data recorder, an AD7891-1 ADC was used to convert the signal received by one of the hydrophones to digital form. The converted data were passed to the implemented TMS320 C6711 DSK receiver for succeeding processing. Since there was only one set of data available to the receiver, the EGC diversity technique was not employed in this situation. A snapshot of the resolved NTOU logo image by the receiver is shown in Fig. 23, where the received waveform is also illustrated. As one can see, the quality of the resolved image in Fig. 23 is comparable to that shown in Fig. 21(b). This justifies the correctness and the effectiveness of the implemented TMS320 C6711 DSK receiver.

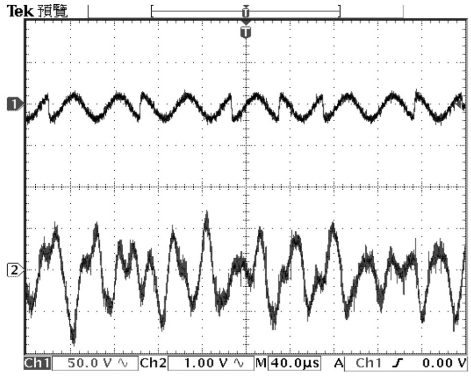

Fig. 22. The transmitted and the received waveforms in the image experiment.

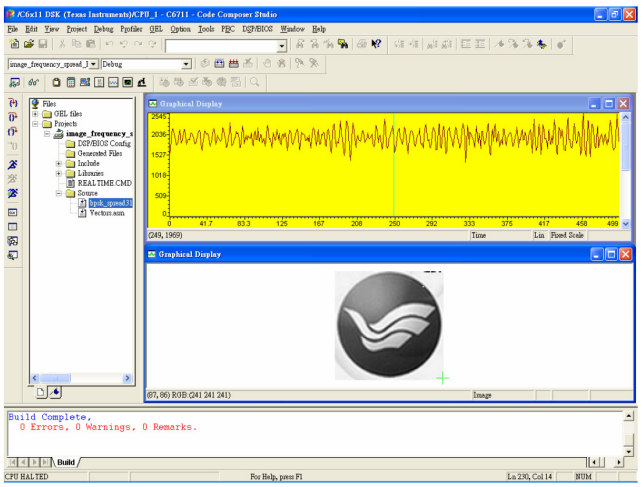

Fig. 23. The received waveform (top) and the resolved image (bottom) by the implemented TMS320 C6711 DSK receiver.

VII. CONCLUSION

Unlike terrestrial wireless communications in which data is transmitted by means of the electromagnetic wave, underwater communications use the acoustic wave instead. The propagation characteristics of the acoustic wave create a challenging environment for establishing reliable data transmissions. In this paper, an all-digital real-time UWA transceiver is proposed. The main contribution of this paper is that it integrates many state-of-the-art digital communication and signal processing techniques into one working UWA transceiver, efficiently implements the transceiver on DSK modules, and successfully tests the implementation in real-time data transmissions over an experimental UWA channel. Specifically, the DS/SS, the EGC diversity, the DD-DFE equalization, and the BCH channel coding techniques are utilized by the transceiver to achieve effective communications through the UWA channel. The proposed transceiver is implemented on two TMS320 C6711 DSK modules, one as the transmitter and the other as the receiver. The implementation for the transceiver is simple yet effective. The goodness of the implemented transmitter is tested

by real-time data transmissions through an experimental water tank mimicking the actual UWA channel. The test result indicates that, although the water tank suffers from severe reverberations, reliable data transmissions can still be accomplished by the proposed transceiver.

Due to the lack of precise knowledge of the acoustic propagation properties (such as time spreading, reverberation, etc.) of the water tank channel, we don't have an appropriate mathematical model for it. Therefore, we are unable to compare the experimental result to the theoretical one. In addition, the test environment is not quite the same as a real UWA channel which may exhibit frequency selective fading and time-varying characteristics. Further field tests of the transceiver are required before we can say more about its performance. These will be the main challenges for our future research.

REFERENCES

1. Choi, Y., Kim, S.-M., Park, J.-W., Lim, Y.-K., and Ko, H.-L., "A Digital Acoustic Transceiver for Underwater Communication without PLL and DLL," *Proceeding of IEEE Oceans Conference*, Vol. 4, pp. 1781-1785 (2003).
2. Choi, Y., Park, J.-W., Kim, S.-M., and Lim, Y.-K., "A Phase Coherent All-Digital Transmitter and Receiver for Underwater Acoustic Communication Systems," *Proceeding of the 35th Southeastern Symposium on System Theory*, pp. 79-83 (2003).
3. Freitag, L., Stojanovic, M., Singh, S., and Johnson, M., "Analysis of Channel Effects on Direct-Sequence and Frequency-Hopped Spread-Spectrum Acoustic Communication," *IEEE Journal of Oceanic Engineering*, Vol. 26, No. 10, pp. 586-593 (2001).
4. Gifford, S., Kleider, J. E., and Chuprun, S., "Synchronization Improvements in Software Defined Radios from the Use of Diversity," *Proceeding of the 21st Century Military Communications Conference*, Vol. 2, pp. 1109-1113 (2000).
5. Haykin, S., *Adaptive Filter Theory*, *4th ed.*, Prentice-Hall (2002).
6. Kilfoyle, D. B. and Baggeroer, A. B., "The State of the Art in Underwater Acoustic Telemetry," *IEEE Journal of Oceanic Engineering*, Vol. 25, No. 1, pp. 4-27 (2000).
7. Labat, J., "Real Time Underwater Communications," *Proceeding of IEEE Oceans Conference*, Vol. 3, pp. 501-506 (1994).
8. Loubet, G., Capellano, V., and Filipiak, R., "Underwater Spread-Spectrum Communications," *Proceeding of IEEE Oceans Conference*, Vol. 1, pp. 574-579 (1997).
9. Lu, F.-S., Tseng, C.-H., Chen, L.-W., Chen, C.-C., and Wu, B.-C., "A Design of Synchronization and Equalization Subsystems for an All-Digital Underwater Pager," (in Chinese), *Proceeding of the Sixth Conference on UnderSea Technology* , pp. 81-90 (2004).
10. Peterson, R. L., Ziemer, R. E., and Borth, D. E., *Introduction to Spread-Spectrum Communication*, Prentice Hall (1995).
11. Rappaport, T. S., *Wireless Communications Principles and Practice*, *2nd Ed*., Prentice-Hall (2002).
12. Sozer, E. M., Proakis, J. G., Stojanovic, R., Rice, J. A., Benson, A., and Hatch, M., "Direct Sequence Spread Spectrum Based Modem for Underwater Acoustic Communication and Channel Measurements," *Proceeding of IEEE Oceans Conference*, Vol. 1, pp. 228-233 (1999).
13. Stojanovic, M., "Recent Advances in High-Speed Underwater Acoustic Communications," *IEEE Journal of Oceanic Engineering*, Vol. 21, No. 4, pp. 125-136 (1996).
14. Stojanovic, M. and Freitag, L., "Hypothesis-Feedback Equalization for Direct-Sequence Spread-Spectrum Underwater Communications," *Proceeding of IEEE Oceans Conference*, Vol. 1, pp. 123-129 (2000).
15. Stojanovic, M., Proarkis, J. G., Rice, J. A., and Green, M. D., "Spread Spectrum Underwater Acoustic Telemetry," *Proceeding of IEEE Oceans Conference*, Vol. 2, pp. 650-654 (1998).
16. Su, S. L. and Yen, N. Y., "Performance of Combined DDLL and AGC Loop for Direct- Sequence Spread-Spectrum Systems," *IEEE Transactions on Communications*, Vol. 48, No. 9, pp. 1455-1458 (2000).
17. Texas Instruments, *TMS320C6000 Peripherals Reference Guide*, TI Literature Number: SPRU190D (2001).
18. Trubuil, J., Le Gall, T., Lapierre, G., and Labat, J., "Development of a Real-Time High Data Rate Acoustic Link," *Proceeding of IEEE Oceans Conference and Exhibition*, Vol. 4, pp. 2159-2164 (2001).
19. Tseng, C.-H., Lu, F.-S., Chen, F.-K., and Wu, S.-T., "Compensation on Multi-Path Fading in Underwater Spread-Spectrum Communication Systems," *Proceeding of IEEE International Symposium on Underwater Technology*, pp. 453-458 (1998).
20. Tsimenidis, C. C., Hinton, O. R., Adams, A. E., and Sharif, B. S., "Underwater Acoustic Receiver Employing Direct-Sequence Spread Spectrum and Spatial Diversity Combining for Shallow-Water Multiaccess Networking," *IEEE Journal of Oceanic Engineering*, Vol. 26, No. 10, pp. 594-603 (2001).
21. Vesma, J. and Saramaki, T., "Interpolation Filters with Arbitrary Frequency Response for All-Digital Receivers," *Proceeding of IEEE International Symposium on Circuits and Systems*, Vol. 2, pp. 568 -571 (1996).
22. Yagnamurthy, N. K. and Jelinek, H. J., "A DSP Based Underwater Communication Solution," *Proceeding of IEEE Oceans Conference*, Vol. 1, pp. 120 – 123 (2003).
23. Yang, T. C., "Differences Between Passive-Phase Conjugation and Decision-Feedback Equalizer for Underwater Acoustic Communications," *IEEE Journal of Oceanic Engineering*, Vol. 29, No. 2, pp. 472-487 (2004).